Sensors & Transducers, Vol. 175, Issue 7, July 2014, pp. 16-21

Sensors & Transducers

A Novel Attitude Measurement Algorithm in Magnetic Interference Environment

[1] Lingxia Li, [*1] Lili Shi, [2] Yu Liu, [1] Zengshan Tian, [1] Mu Zhou

[1] Institute of Communication and Information Engineering, Chongqing University of Posts and Telecommunications, Chongqing 400065, China

[2] Institute of Optical Communication Technology, Chongqing University of Posts and Telecommunications, Chongqing 400065, China

[*1] Tel.: 13883717506, fax: 023-62487972

[*1] E-mail: slili2012@sina.com

Received: 23 April 2014 /Accepted: 30 May 2014 /Published: 31 July 2014

Abstract: The approach of using Magnetic Angular Rate Gravity (MARG) sensor for the current multi-sensor based pedestrian navigation algorithm magnetometers is susceptible to the external magnetic interference. The result of attitude is affected by many factors, like the low-precision MEMS gyro drift and large body linear acceleration measurements. In this paper, we propose anti-jamming algorithm which is based on four elements of Extended Kalman Filtering (EKF). To reduce carrier linear acceleration and local magnetic field that impact on attitude measurement, the adaptive covariance matrix structure is considered. Moreover, the heading angle correction threshold method is used in magnetic field compensation and interference environment. Based on the experimental results, the effectiveness of the proposed algorithm suppresses the influence of the external magnetic interference on heading angle, as well as improving the accuracy of system attitude measurement.

Keywords: Multi-sensor, Complex environment, Fusion algorithm, Anti-magnetic interference.

1. Introduction

The widespread dissemination of smartphones has prompted a great success of positioning systems using mobile terminals for location based services, like the emergency relief map for in-door intelligent navigation construction of city life [1-3]. Magnetic Angular Rate Gravity (MARG) sensor which is based on micro-electro mechanical system (MEMS) technology has been widely applied to intelligent terminals. Hence, the design of MARG positioning system gradually becomes a hot topic [4]. MARG positioning system is with the advantages of low cost, self-positioning, high positioning accuracy, and good stability in short time duration. Due to the sensor noise and cumulative errors, MARG positioning system cannot provide long-term stable and reliable location information.

To solve this problem, an optimal fusion of MARG sensor is justifiable. The MARG sensor based on quaternions Extended Kalman Filtering (EKF) was adopted for attitude algorithm in [5]. The Kalman Filtering (KF) based on quaternion is used for real-time human motion tracking in [6]. In [6], the QUEST algorithm was used instead of Gauss-Newton algorithm. In [7] and [8], to make a progress in improving the accuracy of MARG sensor attitude measurement, the EKF based on four elements was considered. On this basis, the sensor mode which introduced sensor bias compensation and adaptive measurement noise covariance matrix structure

to improve the accuracy of measurement of attitude was established by Liu in Tsinghua University in [9].

The precision of magnetometer is especially important to the attitude measuring accuracy since MEMS gyro error spreads rapidly with respect to time duration. Although the above mentioned algorithms can calculate carrier's attitude, they do not consider the situation that the actual measurements could be influenced by interference. When there is interference magnetic field, the magnetometer data could be resulted into great error attitude solution. In this paper, the anti-jamming algorithms based on quaternion EKF is proposed to reduce the influence of linear acceleration and carriers around the local magnetic field on attitude measurement by constructing an adaptive covariance matrix. Moreover, based on the magnetic field compensation and threshold in magnetic interference environment, the heading angle is corrected and the errors generated from the external interference fields are suppressed effectively.

2. Attitude Measurement and Analysis

The measurement data from inertial measurement unit, like the gyroscope, magnetometer, and accelerometer, are defined as body coordinate frame b. The origin of coordinates is the center of body's gravity and the three coordinate axes are corresponding to the longitudinal axis of the carrier, the horizontal axis, and the vertical axis respectively. The absolute coordinate frame is named by navigation frame, notated as n. The transformation is achieved by quaternion and Euler angle method. The quaternion has been widely used since it can solve singular problem [10].

The conversion relationship between body coordinate frame and navigation frame is shown in (1):

$$\begin{bmatrix} x_b \\ y_b \\ z_b \end{bmatrix} = T_n^b(q) \begin{bmatrix} x_n \\ y_n \\ z_n \end{bmatrix}, \tag{1}$$

where

$$q = q_0 + q_1 i + q_2 j + q_3 k \tag{2}$$

$$T_n^b(q) = \begin{bmatrix} q_0^2+q_1^2-q_2^2-q_3^2 & 2(q_1q_2+q_0q_3) & 2(q_1q_3-q_0q_2) \\ 2(q_1q_2-q_0q_3) & q_0^2-q_1^2+q_2^2-q_3^2 & 2(q_2q_3+q_0q_1) \\ 2(q_1q_3+q_0q_2) & 2(q_2q_3+q_0q_1) & q_0^2-q_1^2-q_2^2-q_3^2 \end{bmatrix} \tag{3}$$

If the rotation quaternion q is obtained, each element, $T_n^b(q)$, can be determined by (3).

When the three-axis gyro angular velocity and initial attitude are obtained, the differential equation of attitude quaternion is as follows:

$$\begin{cases} q(t_0) = q_0 \\ \dfrac{d}{dt}q = \dfrac{1}{2} q \otimes \omega \end{cases}, \tag{4}$$

where the argument t_0 is the initial time of body movement. q_0 is the initial alignment attitude quaternion. Notation " $\otimes$ " is the quaternion multiplication sign. ω is the posture angular velocity vector which is defined in (5):

$$\omega = \begin{bmatrix} 0 & -\omega_x & -\omega_y & -\omega_z \\ \omega_x & 0 & \omega_z & -\omega_y \\ \omega_y & -\omega_z & 0 & \omega_x \\ \omega_z & \omega_y & -\omega_x & 0 \end{bmatrix} \tag{5}$$

Within the time sampling interval T, the angular rate can be assumed to be a fixed value, where T is also recognized as the update interval of rotation quaternion. On this basis, the attitude quaternion model in discrete time condition can be expressed in (6):

$$q_{k+1} = \exp(\omega T) q_k, (k = 0,1,\cdots) \tag{6}$$

Therefore, the attitude rotation matrix is updated by (6) and (2) based on the angular velocity data from three-axis gyroscope.

3. EKF Design

EKF is proposed to do sensor data fusion. The process of EKF is defined in (7):

$$\begin{cases} x_{k+1} = Ax_k + w_k \\ y_k = Cx_{k+1} + v_k \end{cases}, \tag{7}$$

where w_k is the covariance matrix vector of process noise. v_k is the measurement noise covariance matrix vector. According to the discrete-time model of gyro quaternion method, the state transition vector equation is defined as

$$q_{k+1} = Aq_k + w_k, \tag{8}$$

where $A = \exp(\frac{1}{2}\Omega(\omega T))$ is state transition matrix.

The process noise covariance matrix Q_k is

$$Q_k = \begin{bmatrix} \sigma_\omega^2 I & 0 & 0 \\ 0 & \sigma_g^2 I & 0 \\ 0 & 0 & \sigma_g^2 I \end{bmatrix} \quad (9)$$

The observation equation is constructed by stacking accelerometer and magnetometer measurement vectors, such that

$$y_k = \begin{bmatrix} \boldsymbol{a}_{k+1} \\ \boldsymbol{m}_{k+1} \end{bmatrix} = \begin{bmatrix} T_n^b(q_{k+1}) & \mathbf{0} \\ \mathbf{0} & T_n^b(q_{k+1}) \end{bmatrix} \begin{bmatrix} \boldsymbol{g} \\ \boldsymbol{h} \end{bmatrix} + \begin{bmatrix} {}^a v_k \\ {}^m v_k \end{bmatrix}, \quad (10)$$

where $T_n^b(q_{k+1})$ is the attitude rotation matrix of quaternion updated; $\boldsymbol{g}$ is the gravitational acceleration vector; $\boldsymbol{h}$ is the magnetic field intensity vector. The covariance matrix of measurement model R_k is

$$R_k = \begin{bmatrix} \sigma_a^2 I & 0 \\ 0 & \sigma_m^2 I \end{bmatrix} \quad (11)$$

Due to the nonlinear relationship between state and measurement vectors, (11) can be obtained as a linearized observation matrix, as shown in (12).

$$C = \begin{bmatrix} -2q_2 & 2q_3 & -2q_0 & 2q_1 \\ 2q_1 & 2q_0 & 2q_3 & 2q_2 \\ 4q_0 & 0 & 0 & 4q_3 \\ 2b_y q_3 - 2b_z q_2 & 2b_y q_2 + 2b_z q_3 & 2b_y q_1 - 2b_z q_0 & 2b_y q_0 + 2b_z q_1 \\ 4b_y q_0 + 2b_z q_1 & 2b_z q_0 & 4b_y q_2 + 2b_z q_3 & 2b_z q_2 \\ -2b_y q_1 + 4b_z q_0 & -2b_y q_0 & 2b_y q_3 & 2b_y q_2 + 4b_z q_3 \end{bmatrix} \quad (12)$$

In the stationary state, the body tilt angle of relative plane can be calculated by accelerometer accurately. By using the actual output value of accelerometer directly when the body gets linear acceleration, the body attitude angle results in a large error. Therefore, the estimator constructs a new data covariance by an adaptive method, as shown in (13).

$$\sigma_a^2 = (\| \mathbf{a}_k \| - \| \mathbf{g} \|) \quad (13)$$

The proposed system can be adjusted to the weight of measured value in a real-time manner. The covariance changes with the change of the body producing a larger linear acceleration.

A large error of magnetometer measurements appears when the ambient magnetic interference exists. Interference caused by magnetometer is normally modified by magnetic field compensation, while the external magnetic interference which is random and difficult to be eliminated cannot be compensated previously [11]. To solve this problem, we construct an adaptive covariance σ_m^2 as

$$\sigma_m^2 = k_{m1}(\| m_k \| - \| m_0 \|) + k_{m2} var(\| m_{k\text{-}N} \| : \| m_{k+N} \|), \quad (14)$$

where k_{m1} and k_{m2} are the setting weighting factors. $var(\| m_{k\text{-}N} \| : \| m_{k+N} \|)$ is the variance modulo value that each point of the magnetometer measurements. m_0 is the local magnetic field strength standard. When the variance is large, the external magnetic interference magnetometer modulus value and modulus values also become large, as well as the covariance.

4. Magnetic Interference Analysis

4.1. Magnetic Field Compensation

To eliminate elliptic differential effect of magnetic compass which is generated by environmental magnetic interference, the initial calibration of magnetometer before movement is considered in [12]. Without considering the situation that the vector magnetic field and measurement error exist, the body movement is with small change in magnetic field area. For the strap-down magnetic sensor, the horizontal component of geomagnetic field trajectory measurement is a circle on the X and Y shaft, the circle is centered on the origin, and the radius is the horizontal intensity of geomagnetic field [13-14]. The trajectory can be approximately recognized as an ellipse while actual magnetic sensor measurement, for there are many kinds of measurement error and the magnetic interference existing, which will cause the center of the circle shift, thus the shape distorted, as shown in Fig. 1.

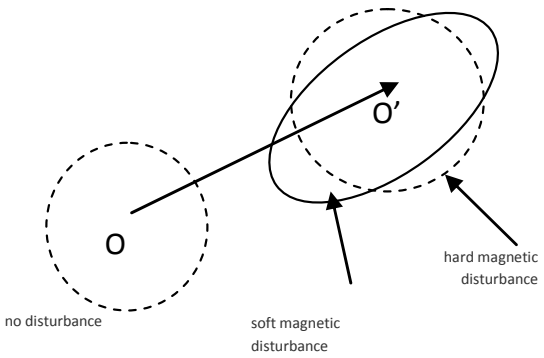

Fig. 1. 2D magnetic field trajectory measured by strap-down magnetometer.

In this paper, the 8 characters calibration method is used to determine the maximum and minimum of three-axis magnetometer data before body movement, and meanwhile the three-axis calibration

factor and bias value are obtained, as shown in (15) and (16).

$$\begin{cases} X_{zero} = (X_{\max} - X_{\min})/2 \\ Y_{zero} = (Y_{\max} - Y_{\min})/2 \\ Z_{zero} = (Z_{\max} - Z_{\min})/2 \end{cases}, \quad (15)$$

$$\begin{cases} K_x = \max\{1, X_{zero}/(X_{zero} - X_{\max})\} \\ K_y = \max\{1, Y_{zero}/(Y_{zero} - Y_{\max})\} \\ K_z = \max\{1, Z_{zero}/(Z_{zero} - Z_{\max})\} \end{cases}, \quad (16)$$

where X_{zero}, Y_{zero}, and Z_{zero} stand for the three-axis magnetometer bias values. K_x, K_y, and K_z are the three-axis magnetometer calibration factor respectively. The output of the three-axis magnetometer is as follows.

$$\begin{cases} X = K_x \bullet X_{\text{in}} + X_{zero} \\ Y = K_y \bullet Y_{\text{in}} + Y_{zero} \\ Z = K_z \bullet Z_{\text{in}} + Z_{zero} \end{cases} \quad (17)$$

4.2. Threshold Limit

The influence can be normally eliminated by magnetic field compensation algorithm when the outside interference field is stable. The magnetometer data cannot be effectively corrected by magnetic field compensation algorithm when the external magnetic field change is large. Then, a threshold value method for heading correction is proposed in this paper.

The existence of interference is determined by the preprocessing of three axis magnetometer modulus values. With magnetometer molding and its change rate to judge whether there is a magnetic disturbance. The equations are expressed as follows.

$$\begin{cases} var(\| m_{\text{step-N}} \| : \| m_{\text{step+N}} \|) < 1 \\ |\| m_0 \| - \| m_{\text{step}} \|| < 0.3 \times \| m_0 \| \end{cases}, \quad (18)$$

where $var(\| m_{\text{step-N}} \| : \| m_{\text{step+N}} \|)$ is the variance of magnetometer measurements modulo value for each step. The size of sliding window equals to 2N. $\| m_{\text{step}} \|$ is the modulus value of three-axis magnetometer for each step.

If the relations in (18) are satisfied, the change of magnetometer field strength measurement is not dramatic, the external magnetic interference is not significant, and the attitude angle solved by EKF is optimal. Otherwise, the attitude angle solved by EKF cannot be reliable. The influence of the external magnetic interference on attitude angle is reduced by the incremental attitude angle which is solved by gyro.

In the unstable interference environment, the magnetic field compensation algorithm is ineffective, especially for the local magnetometer with the data varying remarkably, like the shopping malls and garages. The attitude angle solved by gyro is not affected by magnetic interference, but it is credible only in a short time due to cumulative error. Therefore, the heading angle is optimized by the differences between every two neighboring step headings which are solved by gyro, as shown in (19).

$$\begin{cases} y_{ave}(i) = \Delta y_{gyro}(i) + y_{EKF}(i-1) \\ \Delta y_{gyro}(i) = y_{gyro}(i) - y_{gyro}(i-1) \end{cases}, \quad (19)$$

where $\Delta y_{gyro}(i)$ is the heading angle solved by gyro for the current step. $y_{EKF}(i-1)$ is the heading angle solved by EKF for the previous step. $y_{ave}(i)$ is the optimal estimated heading angle.

5. Experimental Results

In our experiments, a Huawei smartphone is selected as the test platform, as shown in Fig. 2. By using Android operating system, the smartphone is integrated with MARG sensors containing a three-axis accelerometer sensor LIS3DH, a three-axis magnetometer sensor akm8963, and a three-axis gyroscope ST L3G4200D. The raw data from MARG sensor are obtained from the Application Program Interface (API) provided by the system with frequency of 50 Hz.

Fig. 2. Sensor data acquisition platform.

In a corridor environment in our university campus, the pedestrian walks along a line in the corridor which is closed rectangle.

We can use the magnetometer over extended periods of time in magnetically stable environments. The stability of an environment is characterized by low ferrous objects, or power-line nearby the

magnetometer. In complicated indoor areas, the problem of navigating a pedestrian becomes even more challenging, due to the proximity to metallic objects and walls, supported by ferrous pillars.

The magnetometer modulus value can clearly reflect the change of the magnetic field. In the magnetic interference area, the magnetometer modulus value is rather changeable.

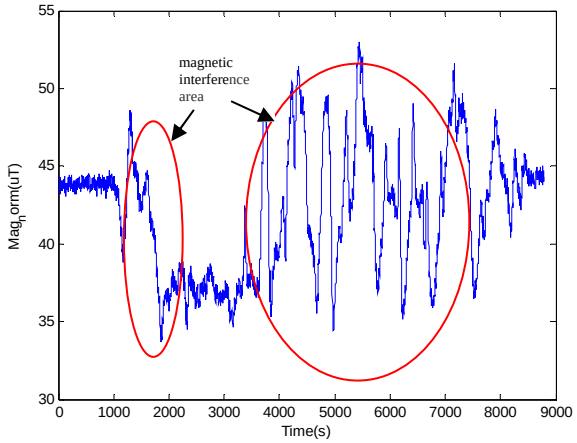

Fig. 3. Curves of three axis magnetometer modulus values.

Fig. 3 shows that there is strong magnetic interference in the environment. Inside the two circles there is a large change of the magnetometer modulus value. In this case, the sensor data are optimized by interference algorithm and EKF. We compare the results of heading angles among EKF, the anti-jamming, and reference in Fig. 4.

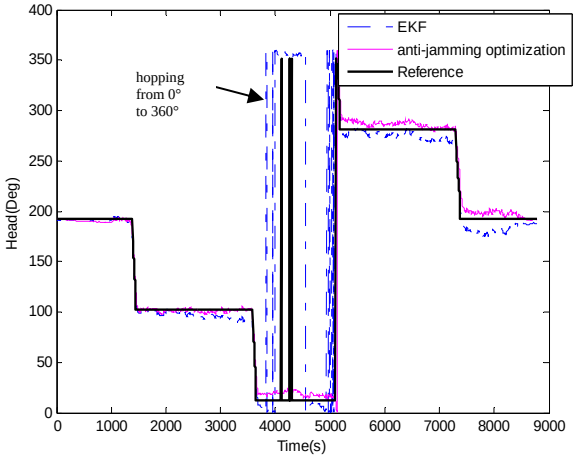

Fig. 4. Comparison of heading angles.

In Fig. 4, the dotted line, thin solid line, and thick solid line indicate the heading angle by EKF, heading angle by EKF with interference, and the real heading angle respectively. The heading angle produces a hopping from 0° to 360° when the pointing due south or north direction. The results in Fig. 4 show that the heading angle by EKF results in large errors, while the errors can be suppressed effectively by our proposed anti-jamming algorithm, especially in the environment with strong magnetic field interference.

Fig. 5 shows that in magnetic interference environment, the value of attitude determination algorithm is much close to the real value inside the circle.

The maximum deviation of heading angles between the anti-jamming algorithm prediction and reference values is within ±15 deg, and average deviation is about 2.67 deg. The heading angles from EKF have large enough error.

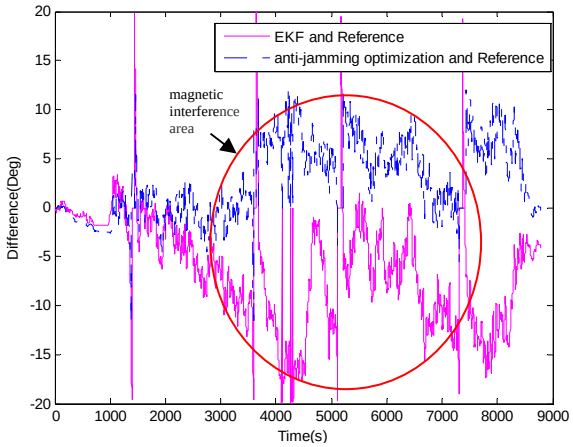

Fig. 5. Difference between EKF and anti-jamming.

6. Conclusions

In this paper, the proposed anti-jamming algorithm based on EKF reduces the influence of the local magnetic field on attitude measurement. A new structure of adaptive covariance matrix using modulus value and variance method is also addressed to solve the problem of the heading errors in magnetic interference environment. The proposed technique has many advantages over any other conventional method such as the use of the threshold limit values, which does not need any error modeling or awareness of the nonlinearity. The algorithm of anti-jamming techniques decreased the required time for the fixing up interference process, extending the opportunity to apply the proposed algorithm in real-time applications. This technique would help decrease the heading errors of the users in pedestrian navigation. Furthermore, in magnetic interference environment, the methods of magnetic field compensation and heading angle correction effectively improve the accuracy of attitude measurement system.

Acknowledgements

This work was supported in part by the Program for Changjiang Scholars and Innovative Research Team in University (IRT1299), National Natural Science Foundation of China (61301126), Special Fund of Chongqing Key Laboratory (CSTC), Fundamental and Frontier Research Project of Chongqing (cstc2013jcyjA40032, cstc2013jcyjA40034, cstc2013jcyjA40041), Scientific and Technological Research Program of Chongqing Municipal Education Commission (KJ130528), Startup Foundation for Doctors of CQUPT (A2012-33), Science Foundation for Young Scientists of CQUPT (A2012-77), and Student Research Training Program of CQUPT (A2013-64).

References

[1]. Hightower J., Borriello G., A survey and taxonomy of location systems for ubiquitous computing, *IEEE Computer*, 34, 8, 2001, pp. 57-66.

[2]. Lee S., Kim B., Kim H., *et al.*, Inertial sensor-based indoor pedestrian localization with minimum 802.15. 4a configuration, *IEEE Transactions on Industrial Informatics*, 7, 3, 2011, pp. 455-466.

[3]. Chon J., Cha H., Lifemap: A smartphone-based context provider for location-based services, *IEEE Pervasive Computing*, 10, 2, 2011, pp. 58-67.

[4]. Woodman O., Harle R., Pedestrian localisation for indoor environments, in *Proceedings of the 10th International Conference on Ubiquitous Computing*, 2008, pp. 114-123.

[5]. Marins J. L., Yun X., Bachmann E. R., *et al.*, An extended Kalman filter for quaternion-based orientation estimation using MARG sensors, in *Proceedings of the IEEE/RSJ International Conference on Intelligent Robots and Systems*, 4, 2001, pp. 2003-2011.

[6]. Yun X., Bachmann E. R., McGhee R. B., A simplified quaternion-based algorithm for orientation estimation from earth gravity and magnetic field measurements, *IEEE Transactions on Instrumentation and Measurement*, 57, 3, 2008, pp. 638-650.

[7]. Strohrmann C., Harms H., Tröster G., et al., Out of the lab and into the woods: Kinematic analysis in running using wearable sensors, in *Proceedings of the 13th International Conference on Ubiquitous Computing*, 2011, pp. 119-122.

[8]. Munguia R., Grau A., An attitude and heading reference system (AHRS) based in a dual filter, in *Proceedings of the IEEE 16th Conference on Emerging Technologies & Factory Automation (ETFA)*, 2011, pp. 1-8.

[9]. Liu Xingchuan, Zhang Sheng, Li Lizhe, *et al.*, Measurement algorithm based on quaternion attitude MARG sensor, *Tsinghua University: Natural Science*, 52, 5, 2012, pp. 627-631.

[10]. Li F., Zhao C., Ding G., *et al.*, A reliable and accurate indoor localization method using phone inertial sensors, in *Proceedings of the ACM Conference on Ubiquitous Computing*, 2012, pp. 421-430.

[11]. Ali A., Siddharth S., Syed Z., *et al.*, An Improved Personal Dead-Reckoning Algorithm for Dynamically Changing Smartphone User Modes, in *Proceedings of the 25th International Technical Meeting of the Satellite Division of the Institute of Navigation (ION GNSS 2012)*, Nashville, 2012, pp. 2432-2439.

[12]. Madgwick S. O. H., Harrison A. J. L., Vaidyanathan R. Estimation of IMU and MARG orientation using a gradient descent algorithm, in *Proceedings of the IEEE International Conference on Rehabilitation Robotics (ICORR)*, 2011, pp. 1-7.

[13]. Shin B., Lee J. H., Lee H., *et al.*, Indoor 3D pedestrian tracking algorithm based on PDR using smartphone, in *Proceedings of the 12th International Conference on Control, Automation and Systems (ICCAS)*, 2012, pp. 1442-1445.

[14]. Nilsson J. O., Zachariah D., Skog I., *et al.*, Cooperative localization by dual foot-mounted inertial sensors and inter-agent ranging, *arXiv Preprint arXiv: 1304.3663*, 2013.